# Comparison of ion cyclotron wall conditioning discharges in hydrogen and helium in JET

Y. Kovtun, T. Wauters, D. Matveev, R. Bisson, I. Jepu, S. Brezinsek, I. Coffey, E. Delabie, A. Boboc, T. Dittmar, et al.

Nuclear Materials and Energy 37 (2023) 101521

Contents lists available at ScienceDirect

Nuclear Materials and Energy

journal homepage: www.elsevier.com/locate/nme

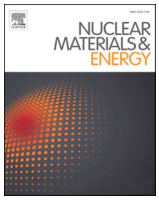

# Comparison of ion cyclotron wall conditioning discharges in hydrogen and helium in JET

Y. Kovtun [a,*], T. Wauters [b], D. Matveev [c], R. Bisson [d], I. Jepu [e], S. Brezinsek [c], I. Coffey [e], E. Delabie [e], A. Boboc [e], T. Dittmar [c], A. Hakola [f], P. Jacquet [e], K. Kirov [e], E. Lerche [g,e], J. Likonen [f], E. Litherland-Smith [e], T. Loarer [h], P. Lomas [e], C. Lowry [e], E. Pawelec [i], C. Perez von Thun [j], A. Meigs [e], M. Maslov [e], I. Monakhov [e], C. Noble [e], S. Silburn [e], H. Sun [e], D. Taylor [e], E. Tsitrone [h], A. Widdowson [e], H. Sheikh [e], D. Douai [h], JET Contributors [1]

[a] Institute of Plasma Physics of the NSC KIPT, Kharkiv, Ukraine
[b] ITER Organization, Route de Vinon-sur-Verdon, CS 90 046, 13067, St Paul Lez Durance Cedex, France
[c] Forschungszentrum Jülich GmbH, IEK-4, Jülich, Germany
[d] Aix-Marseille Univ, CNRS, PIIM, Marseille, France
[e] UKAEA, CCFE, Culham Science Centre, Abingdon, Oxon OX14 3DB, UK
[f] VTT, Espoo, Finland
[g] LPP-ERM/KMS, TEC, Brussels, Belgium
[h] CEA, IRFM, Saint Paul Lez Durance, France
[i] Institute of Physics, Opole University, Opole, Poland
[j] Institute of Plasma Physics and Laser Microfusion, Hery 23, 01-497, Warsaw, Poland

ARTICLE INFO

*Keywords:*
Wall conditioning
Radio-frequency discharge
Tokamak
Plasma production
Ion cyclotron

ABSTRACT

This paper explores the plasma parameters of helium and hydrogen Ion Cyclotron Wall Conditioning (ICWC) discharges performed in JET as part of a He/H fuelling changeover experiment. The conducted study shows that plasma with a higher density is formed in helium than in hydrogen. A distinct glow in the ion cyclotron resonance zone is observed throughout the discharge in He. In H-ICWC discharges, a lower radio-frequency coupling efficiency and coupled power was observed than in He-ICWC discharges. While the helium concentration decreased with the number of H-ICWC pulses and the same for hydrogen in He-ICWC, which is the intended result of the plasma wall interaction in the ICWC changeover procedure, the main features of hydrogen as well as the helium IC discharge do not change dramatically.

## 1. Introduction

Wall conditioning is essential for the operation of tokamaks and stellarators, and thus for the advancement of magnetic confinement fusion research [1–3]. It is applied to overcome several problems. First, to decrease the flux of impurities from the first wall into the confinement volume and, accordingly, to decrease the radiation losses from the plasma. Control of the recycling of hydrogen fuel fluxes and, therefore, plasma density. Removal of tritium from plasma-facing materials for safety. Accelerating the transition from plasma tests with one element or isotope to another. Recovering vacuum conditions after events such as disruptions and vacuum leaks.

Wall conditioning includes various methods [1,2]. One such method is the use of plasma produced by radio-frequency (RF) discharges of various frequency ranges, including the ion-cyclotron frequency range [1–4]. This method has been and is used on stellarators W7-AS [5], U-3M [6], U-2M [7], LHD [8] and tokamaks TEXTOR [9], ASDEX Upgrade [10], TORE SUPRA [11], EAST [12], HT-7 [13], KSTAR [14]. Ion Cyclotron Wall Conditioning (ICWC) is one of the developed methods for fuel removal at JET [3,4,15]. In future it is planned to use ICWC in the superconducting stellarator W7-X [16] and tokamaks DTT [17], ITER [18]. ICWC can use the same antennas as used for ion cyclotron resonance heating (ICRH) without requiring additional hardware. However, the approaches in implementing ICWC and ICRH are quite different. In

* Corresponding author.
*E-mail address:* Ykovtun@kipt.kharkov.ua (Y. Kovtun).
[1] See the author list of 'Overview of JET results for optimising ITER operation' by J. Mailloux et al 2022 Nucl. Fusion 62 042026.

https://doi.org/10.1016/j.nme.2023.101521
Received 11 June 2023; Received in revised form 25 August 2023; Accepted 24 September 2023
Available online 26 September 2023

ICRH methods, RF power is applied to an already made plasma. In ICWC, the discharge is produced and sustained by the RF antenna, with parameters appropriate for wall conditioning procedures. Initial conditions (pressure, magnetic field, etc.) must be selected favorable for RF breakdown as well as for subsequent power coupling in the steady conditioning plasma [19]. The plasma parameters of the ICWC discharge affect the efficiency of wall conditioning. Therefore, ICWC discharge analysis is necessary to optimize the wall conditioning procedure.

Previously, discharge production for ICWC in JET was analyzed for example in [19]. However, the comparison and analysis of the ICWC discharge plasma parameters in different gas atmospheres has not been carried out before. In the present work, we compare the ICWC discharge parameters in hydrogen ($H_2$) and helium (He) atmospheres in JET under nearly identical conditions. The experiments were conducted to investigate the effect of He/H changeover with Be/W walls.

## 2. Experimental details

The JET C43 campaign was initiated with He/H fuelling changeover experiments [20]. The experiments involved two phases. In the first stage, ICWC hydrogen discharges were carried out to decrease the helium concentration within the facility. The hydrogen scenario unfolded as follows: one beryllium monitoring pulse (BeMP), followed by 15 ICWC discharges, another BeMP, and finally 5 diverted plasma pulses (DPP). After that, at the next phase, ICWC is discharged in helium to decrease hydrogen concentration in the facility. The sequence of discharges in helium is as follows: 1 BeMP and 8 ICWC discharges, followed by another 1 BeMP and 9 ICWC discharges, then 1 BeMP and 4 DPP, and finally, 1 BeMP.

The ICRH system at JET includes one ITER-like antenna (ILA) and four A2 antennas known as the 'A', 'B', 'C', 'D' [21–24]. The latter A2 antennas have been used in ICWC experiments [25]. They each include four poloidal straps with a Faraday shield. The present experiment used antenna 'D' to produce the ICWC discharge plasma. The phasings of the antenna straps were 'monopole' (0 0 0 0). The generated RF output power was up to 0.45 MW at a frequency of $f_{RF}$ = 28.24 MHz. The toroidal magnetic field in the center was $B_t = 1.9$ T. In these conditions, the ion cyclotron resonance (ICR) zone for the fundamental harmonic of hydrogen $\omega_{ci}$ ($H^+$) $\approx \omega_{RF} = 2\pi \times f_{RF}$ is localized on the torus axis ~3.04 m. At the same time, for $He^{2+}$ and $He^+$ helium ions, the ICR zone for the first harmonic is outside the plasma volume. Correspondingly, for helium ions $\omega_{RF} \approx 2\omega_{ci}$ ($He^{2+}$) $\approx 4\omega_{ci}$ ($He^+$). In ICWC discharges in hydrogen, there was additionally a vertical magnetic field of magnitude 15 mT. In the two shots, #101044 and #101045 the value of the vertical field was 22.5 and 7.5 mT, respectively. Only four ICWC discharges in helium additionally had a vertical magnetic field 22.5 mT (#101082), 7.5 mT (#101083) and 15 mT (#101084, #101085).

The line integrated density was measured using a multi-channel Far Infrared (FIR) interferometer [26,27] on four vertical channels (see Fig. 1a), with a sensitivity of $3 \times 10^{17}$ particle/m$^2$. Time-resolved optical emission spectroscopy was used to measure the intensities of spectral lines of helium and hydrogen, as well as lines of plasma impurities. In the visible range, the spectrometric systems known as KS3 and KS8 [28] in JET were used. The poloidal cross section of the KS3 viewing geometry is shown in Fig. 1b. The evolution of the ICWC discharge was registered by tangential video diagnostics. Residual gases were analyzed by sub-divertor gas analysis diagnostic [29,30]. The sub-divertor hydrogen concentration was measured by Penning gauge spectroscopy [29,30].

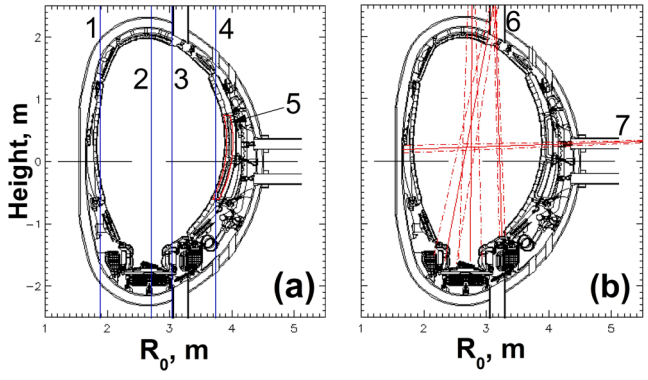


**Fig. 1.** Poloidal cross section of the FIR (a) and spectrometer systems KS3 (b) viewing geometry. 1–4 vertical channels FIR, respectively, LID 1-LID 4; 5 - A2 antenna; 6 and 7 vertical and horizontal view KS3.

## 3. Results and discussion

The ICWC pulse starts by injecting RF power at ≈ 42.8 s, followed by gas injection. The pulse injection of the operating gas was performed with a delay of ~400 ms, relative to the start of the RF generator. At time ≈ 61.9 s, both RF and gas stop. The time of the appearance of a plasma glow in the volume, recorded by a tangential high-speed video camera with a time resolution of 5 ms, was different for ICWC discharges in hydrogen and helium. In H-ICWC discharges, the glow appeared in the interval from ~0.3 to ~0.8 s after the start of gas injection. At the same time in He-ICWC discharges this time was from ~1 to ~2 s. In fact, during this time several processes take place sequentially. Reaching the pressure, concentration of neutral atoms, in the volume necessary for RF breakdown. The pressure of hydrogen and helium in the vacuum vessel at the start of the glow were ~ $(1.7–3) \times 10^{-5}$ mbar and $(0.9–1.7) \times 10^{-4}$ mbar, respectively. The plasma glow that occurs right after breakdown when the plasma density is still low [19,31] is analysed using video diagnostics. The further dynamics of ICWC discharge glow is also different in hydrogen and helium. In H-ICWC discharges the brightest glow near the wall, the intensity of which varies over time (see Fig. 2a, b). Shortly after the discharge initiation in He, the presence of horizontal filaments near the low field side was observed (see Fig. 2c), suggesting that initially, the plasma flows from a localised plasma production zone along the shaped vertical magnetic field configuration. Also, a more intense glow in the ICR zone throughout the discharge in He is observed (see Fig. 2d). Video diagnosis with the $H_\alpha$ filter (656 nm) shows an intense glow of the hydrogen line in the ICR region (see Fig. 3). Both features are not observed in H (see Fig. 2a,b). The presence of a minority addition of hydrogen in the He-ICWC discharges is confirmed by both spectrometric diagnostics and Penning gauge spectroscopy.

In Fig. 4 shows a comparison of the discharge parameters for two pulses in hydrogen and helium. As can be seen in both pulses there are spectral lines of hydrogen and helium. Accordingly, this shows the presence of the minority hydrogen or helium resulting from plasma wall interaction in addition to the main fuelled species. The highest intensity is observed for the spectral lines of the main gas. Significant differences are observed in the achieved plasma density for these discharges. Measurements of the line-integrated electron density along the vertical chord in the H-ICWC discharge showed that the density is below the sensitivity of the interferometer of $3 \times 10^{17}$ m$^{-2}$. In the case of the ICWC discharge in He, the density was higher than $3 \times 10^{17}$ m$^{-2}$. The line-integrated electron density measurements (see Fig. 4 a, c) were made in vertical channels LID 3 (see Fig. 1a) at the radial coordinate $R_0 \approx 3.02$ m, which is very close to the ICR zone ~3.04 m. Correspondingly, the ICR zone also showed an increase in plasma density. The maximum achieved $N_eL$ value was up to $6 \times 10^{17}$ m$^{-2}$. The average density estimate gives a value of $\sim 2 \times 10^{17}$ m$^{-3}$. Higher densities are also observed in the other vertical channels LID 2 ($R_0 \approx 2.69$ m) and LID 4 ($R_0 \approx 3.75$ m) in the He-ICWC discharge. For LID 2 the maximum $N_eL$ was up to $5.3 \times 10^{17}$ m$^{-2}$, LID 4 was up to $3.2 \times 10^{17}$ m$^{-2}$. Accordingly, the entire plasma volume has a higher density in He-ICWC than in H-ICWC discharges.

Fig. 4b,d shows the time evolution of the intensity of the spectral lines of hydrogen, helium, and impurities in the vertical midplane. Just

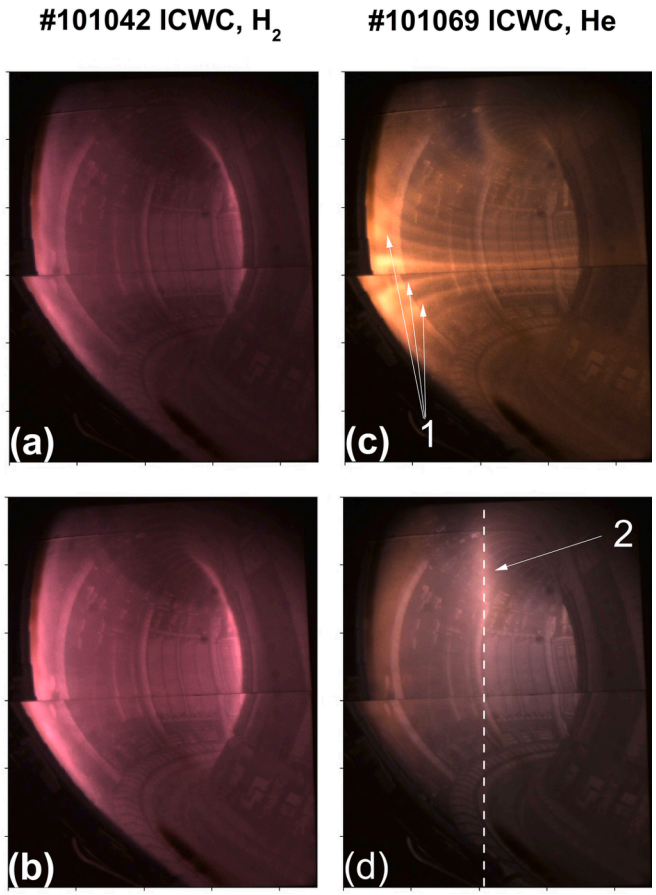


**Fig. 2.** Tangential camera images of a ICWC discharge in $H_2$ (a,b) and He (c, d). Time index 45.9 s (a, c) and 47.6 s (b,d). 1 - horizontal filaments, 2 - emission in ICR zone. The dash line approximates ICR zone position.

as in the horizontal midplane (see Fig. 4a,c), the maximum intensity is observed for the spectral lines of the main gas and lower intensity for the minority additive. In the He-ICWC discharge spectral lines of helium, oxygen, and carbon ions are also observed (see Fig. 4b,d). In H-ICWC discharge the spectral lines of helium and carbon ions are below the detection limit. The intensity of the oxygen spectral line is an order of magnitude lower than in the He-ICWC discharge. This difference may be due to the higher plasma density in the helium discharge. In this case, the flux of particles both helium and including hydrogen [32] to the wall will increase. The plasma-wall interaction will increase accordingly. This will lead to an increase in the flux of impurities in the plasma. The probability of collisions resulting in ionization and excitation of ions will increase with increasing density. Accordingly, the intensity of the spectral lines of the ions should increase. On the other hand, it is also possible that the temperature of the electrons in the helium discharge is higher than in hydrogen.

A difference in coupled RF power for ICWC discharge in hydrogen and helium is also observed (see Fig. 4). Fig. 5 summarizes the RF parameters and line-integrated electron density for ICWC pulses. The efficiency of inputting RF power into the plasma is characterized by coupling efficiency η. The antenna–plasma coupling efficiency is the fraction of the power coupled to the plasma to the power launched at the generator, $\eta = P_{coup}/P_{gen}$ [19]. In H-ICWC discharges, a lower η was observed than in He-ICWC discharges, respectively up to 0.4 and 0.58. Accordingly, the coupled RF power $P_{coup}$ in the H discharge was lower than in the He discharge, up to 0.16 MW and 0.24 MW, respectively. The total coupled energy $W_c$ in the H discharge was lower than in the He discharge, up to 1.2 MJ and 4 MJ, respectively. Higher values of coupling efficiency, respectively $P_{coup}$ and $W_c$ in He-ICWC seem to be associated with a higher plasma density in the volume and other plasma parameters compared to the H-ICWC discharge.

Fig. 6 shows the change in pressure and mass spectra during and after the RF pulse. As can be seen, both the hydrogen and helium pressure increases after the RF pulse. The H-ICWC discharge also shows an increase in the signal on the mass spectrum not only for $H_2$ (m = 2) but also for He (m = 4), HD (m = 3), and $H_2O$ (m = 18). The situation after the He-ICWC discharge is different, where the signals increase only for He (m = 4) and $H_2$ (m = 2). Detailed analysis of the gas balance by mass

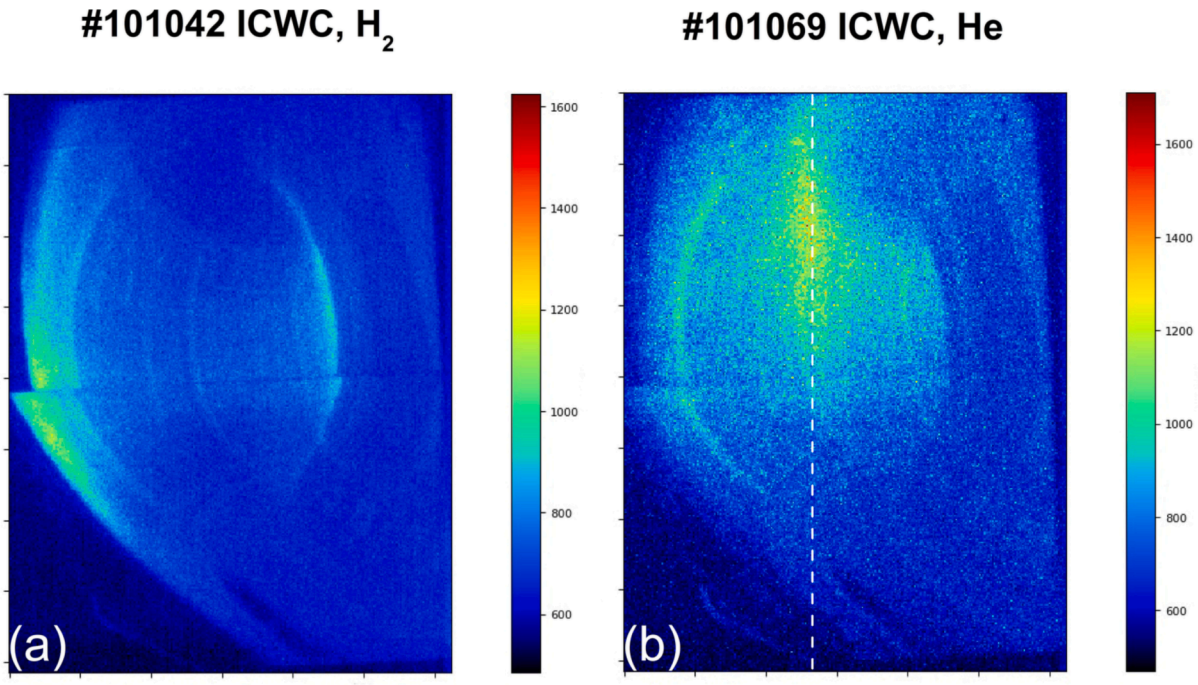


**Fig. 3.** Tangential camera images $H_\alpha$ (656 nm) of a ICWC discharge in $H_2$ (a) and He (b). Time index 47.6 s. The dash line approximates ICR zone position.

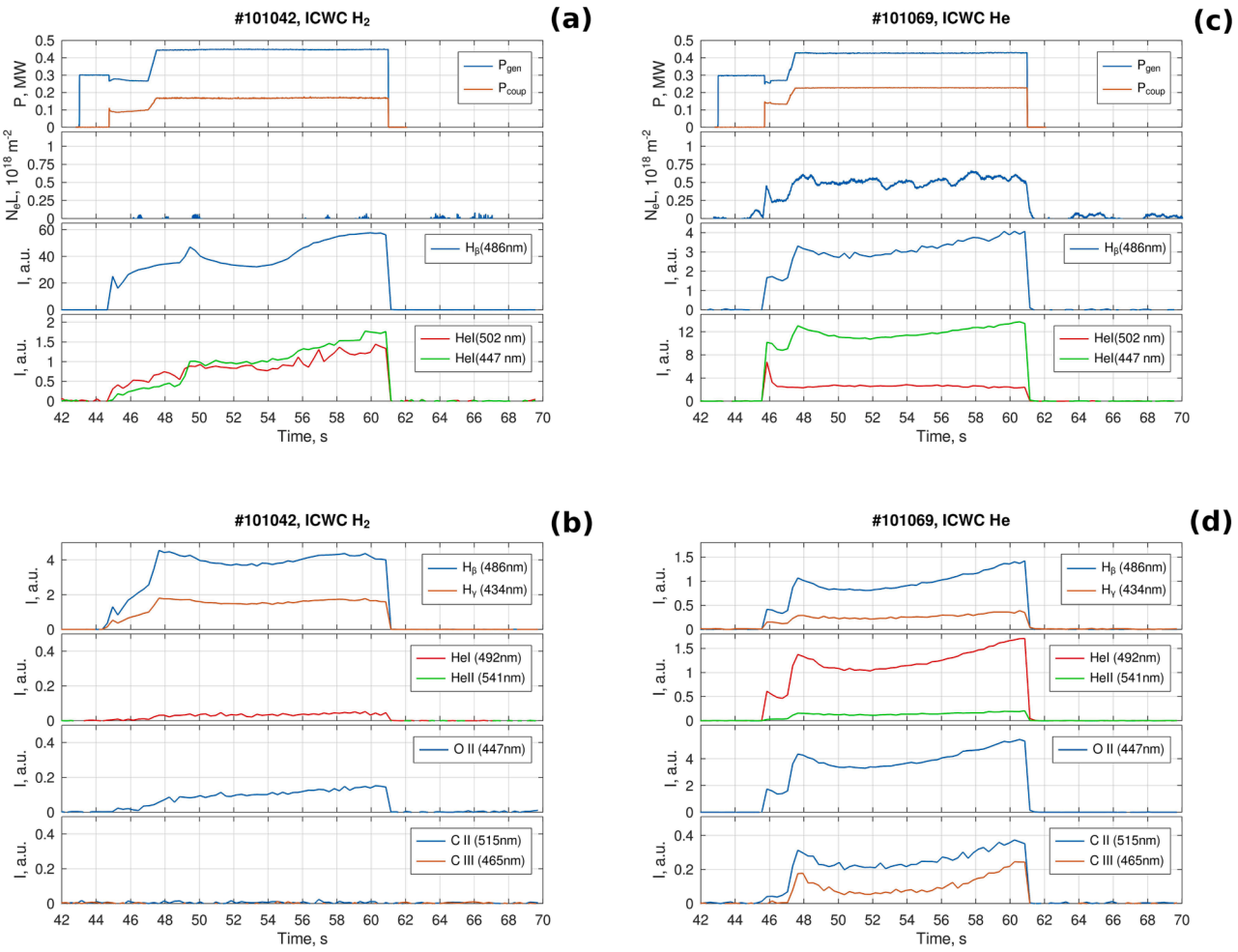


**Fig. 4.** (a, c) Time evolutions of generated $P_{gen}$ and coupled $P_{coup}$ powers, line integrated electron density $N_eL$ (LID 3, see Fig. 1a), optical emission intensities of H I and He I (horizontal midplane, KS 3, see Fig. 1 b).(b, d) Time evolutions of optical emission intensities of H I, He I and He II, O II, C II, C III (vertical, inner divertor, KS 3 see Fig. 1 b). The ICWC discharge in $H_2$ (left), the ICWC discharge in He (right).

spectrometry are available in [20].

Penning gauge spectroscopy show a helium concentration of ~3–9 % in the H-ICWC discharge and ~0.7–6 % of Hydrogen in the He-ICWC discharge. It is observed that the concentration of helium decreases with the number of H-ICWC pulses and the same for hydrogen in He-ICWC. This is the result of the progressing He/H changeover via the interaction of plasma with the wall in the ICWC procedure. Detailed analysis of the changeover between helium and hydrogen fueled plasmas are available in [20].

The differences in hydrogen and helium ICWC discharges in JET seem to be due to the presence of a hydrogen minority additive in helium. A similar result was also observed in D-ICWC with minority $H_2$ and H-ICWC with minority of $D_2$ at JET. In both experiments, three antennas 'A', 'B', and 'D' at ≈ 25 MHz were used to produce plasma. In the D-ICWC experiments with minority $H_2$ the toroidal magnetic field was ≈ 1.65 T and, accordingly, the condition $\omega_{RF} \approx \omega_{ci}$ ($H^+$) ≈ $2\omega_{ci}$ ($D^+$) was satisfied. The hydrogen concentration in the D-ICWC was ~3–9 %. In H-ICWC experiments with minority $D_2$ the magnetic field value was $B_t \approx$ 3.3 T and, accordingly, $\omega_{RF} \approx \omega_{ci}$ ($D^+$), $\omega_{ci}$ ($H^+$) > $\omega_{RF}$. The deuterium concentration was ~8–9 %. In both experiments, a glow was observed in the ICR zone, as can be seen in Fig. 7. As well as a higher plasma density in this region. Thus, in D-ICWC with minority $H_2$ in some pulses the density reached $N_eL \approx 2.7 \times 10^{18}$ $m^{-2}$ (LID 3), while in H-ICWC discharges with minority $D_2$ densities up to $7.4 \times 10^{18}$ $m^{-2}$ (LID 3) have been achieved.

A similar situation is observed in studies of ICRF plasma production with minor additions of hydrogen in helium on Uragan-2M and LHD stellarators [33–37]. In the case of minor additions of $H_2$ in He, the plasma density was higher than in pure hydrogen or helium [35,37]. These differences are explained by the intense heating of the plasma electrons in the mode conversion regime [33]. The results in JET in ICWC discharges with minority additives can be ascribed to the same process.

## 4. Conclusions

This paper explores the plasma and discharge parameters of helium and hydrogen ICWC discharges at JET. The conducted studies of the ICWC discharge show that plasma with a higher density is formed in helium up to $6 \times 10^{17}$ $m^{-2}$, respectively $> 3 \times 10^{17}$ $m^{-2}$, than in hydrogen. Shortly after the discharge initiation in He, the presence of horizontal filaments near the low field side was observed. This indicates that the plasma initially flows from a localized plasma production zone along the barrel shaped configuration of the magnetic field. A more intense glow in the visible range and the hydrogen $H_\alpha$ line in the ICR area throughout the discharge in He is observed. Both features are not observed in H. In H-ICWC discharges, a lower RF coupling efficiency was observed than in He-ICWC discharges, respectively up to 0.4 and 0.58. Accordingly, the coupled RF power in the H discharge was lower than in the He discharge, up to up to 0.16 MW and 0.24 MW respectively. Higher values of coupling efficiency seem to be associated with a higher plasma density in the volume. The difference in ICWC discharges in

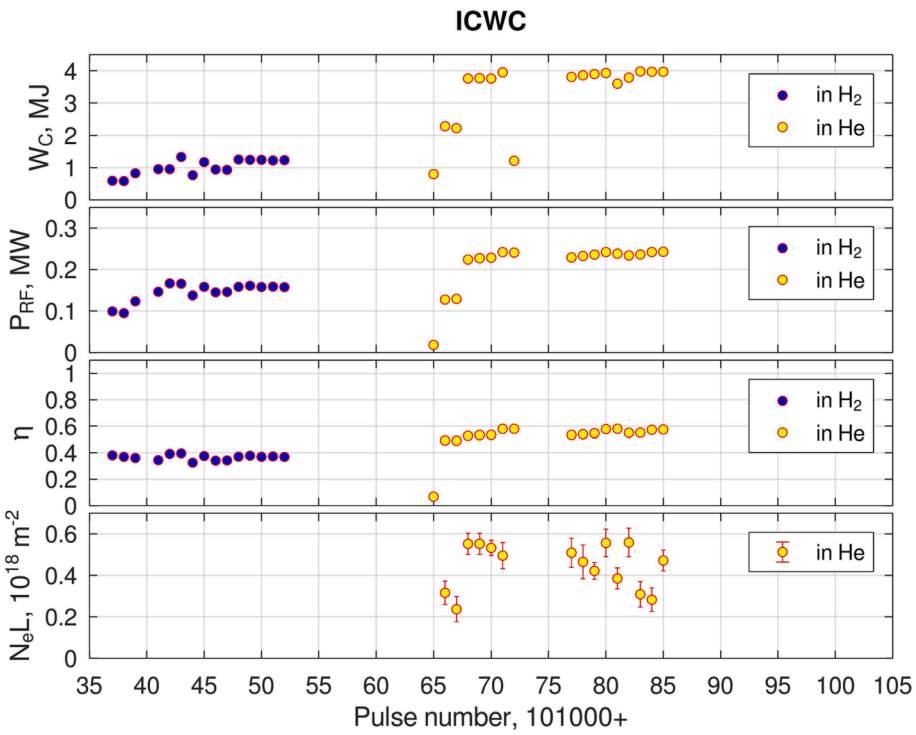


**Fig. 5.** The total coupled energy $W_c$, the average value at the time interval 50–55 s coupled power $P_{coup}$, coupling efficiency η, line integrated electron density $N_eL$ (LID 3, see Fig. 1a).

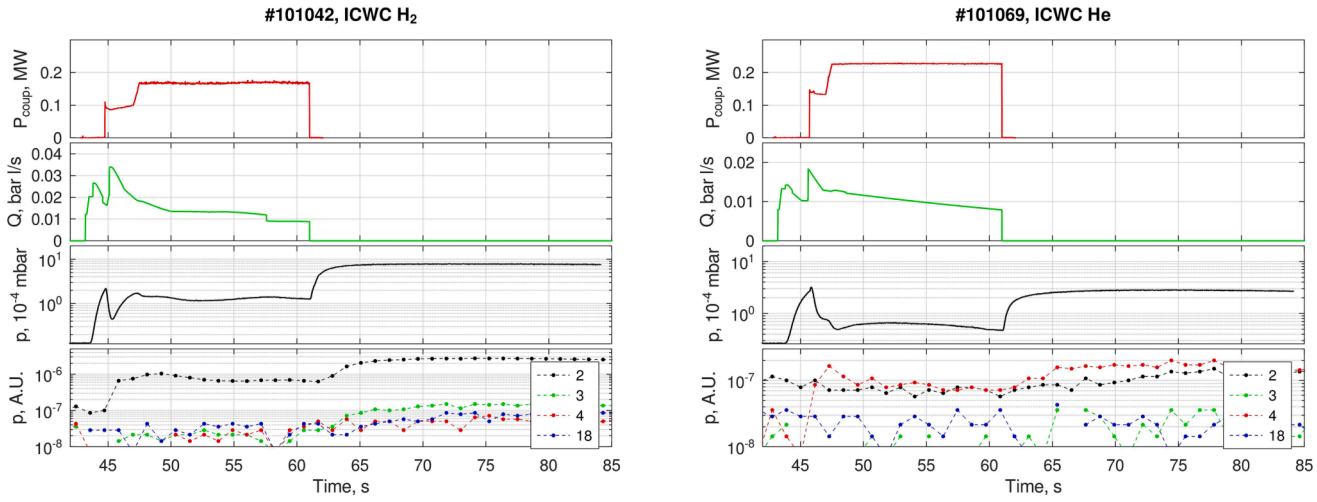


**Fig. 6.** Time evolutions of coupled power $P_{coup}$, gas flow rate Q, pressure p, mass spectrum. The ICWC discharge in $H_2$ (left), the ICWC discharge in He (right).

hydrogen and helium on JET seems to be due to the presence of hydrogen minority additive in helium, and the related possible heating of the plasma electrons in the mode conversion regime.

It is observed that the concentration of helium decreases with the number of H-ICWC pulses and per turn of hydrogen in He-ICWC. Which is the result of He/H changeover in the interaction of plasma with the wall in the ICWC procedure. These results will serve to optimize the wall conditioning procedure and develop an ICWC strategy for superconducting devices.

## CRediT authorship contribution statement

**Y. Kovtun:** Writing – original draft, Visualization, Writing – review & editing, Investigation. **T. Wauters:** Writing – review & editing, Investigation. **D. Matveev:** Investigation. **R. Bisson:** Investigation. **I. Jepu:** Investigation. **S. Brezinsek:** Project administration. **I. Coffey:** Investigation. **E. Delabie:** Investigation. **A. Boboc:** Investigation. **T. Dittmar:** Investigation. **A. Hakola:** Project administration. **P. Jacquet:** Investigation. **K. Kirov:** Investigation. **E. Lerche:** Investigation. **J. Likonen:** Supervision. **E. Litherland-Smith:** Investigation. **T. Loarer:** Supervision. **P. Lomas:** Investigation. **C. Lowry:** Investigation. **E. Pawelec:** Investigation. **C. Perez von Thun:** Investigation. **A. Meigs:** Investigation. **M. Maslov:** . **I. Monakhov:** Investigation. **C. Noble:** Investigation. **S. Silburn:** Investigation. **H. Sun:** Investigation. **D. Taylor:** Investigation. **E. Tsitrone:** Project administration. **A. Widdowson:** Investigation. **H. Sheikh:** Investigation. **D. Douai:** Investigation.

## Declaration of Competing Interest

The authors declare that they have no known competing financial

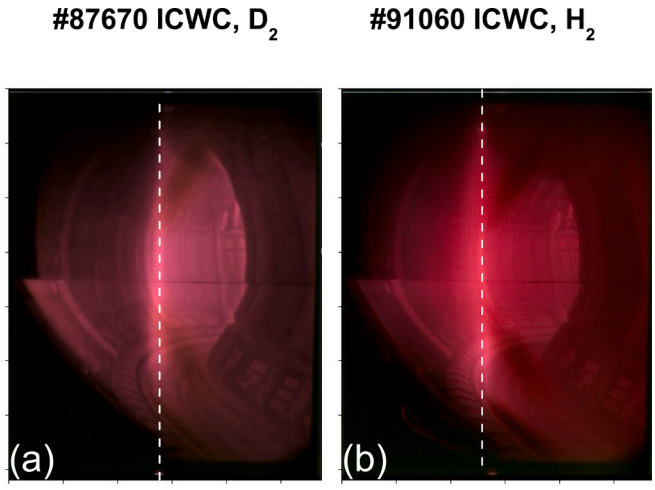


**Fig. 7.** Tangential camera images of a D-ICWC discharge with minority $H_2$ (a) and H-ICWC discharge with minority $D_2$. Time index 45.6 s (a, b). The dash line approximates ICR zone position.

interests or personal relationships that could have appeared to influence the work reported in this paper.

## Data availability

Data will be made available on request.

## Acknowledgements

This work has been carried out within the framework of the EUROfusion Consortium, funded by the European Union via the Euratom Research and Training Programme (Grant Agreement No 101052200 — EUROfusion). Views and opinions expressed are however those of the author(s) only and do not necessarily reflect those of the European Union or the European Commission. Neither the European Union nor the European Commission can be held responsible for them.

This scientific paper has been published as part of the international project co-financed by the Polish Ministry of Science and Higher Education within the programme called 'PMW' for 2022-2023.

The views and opinions expressed herein do not necessarily reflect those of the ITER Organization.

## References

[1] J. Winter, Wall conditioning in fusion devices and its influence on plasma performance, Plasma Phys. Control. Fusion 38 (1996) 1503–1542, https://doi.org/10.1088/0741-3335/38/9/001.
[2] T. Wauters, D. Borodin, R. Brakel, et al., Wall conditioning in fusion devices with superconducting coils, Plasma Phys. Control. Fusion 62 (2020), 034002, https://doi.org/10.1088/1361-6587/ab5ad0.
[3] D. Douai, A. Lyssoivan, V. Philipps, et al., Recent results on Ion Cyclotron Wall Conditioning in mid and large size tokamaks, J. Nucl. Mater. 415 (2011) S1021–S1028, https://doi.org/10.1016/j.jnucmat.2010.11.083.
[4] E. de la Cal, E. Gauthier, Review of radio frequency conditioning discharges with magnetic fields in superconducting fusion reactors, Plasma Phys. Control. Fusion 47 (2005) 197–218, https://doi.org/10.1088/0741-3335/47/2/001.
[5] R. Brakel, D. Hartmann, P. Grigull, ICRF wall conditioning experiments in the W7-AS stellarator, J. Nucl. Mater. 290–293 (2001) 1160–1164, https://doi.org/10.1016/S0022-3115(00)00554-7.
[6] A.V. Lozin, V.E. Moiseenko, L.I. Grigor'eva, et al., Cleaning of inner vacuum surfaces in the Uragan-3M facility by radio-frequency discharges, Plasma Phys. Rep. 39 (2013) 624–631, https://doi.org/10.1134/S1063780X13070052.
[7] Yu. V. Kovtun, V.E. Moiseenko, A.V. Lozin et al., Radio frequency wall conditioning discharges at low magnetic fields in Uragan-2M stellarator, 48th EPS Conference on Plasma Physics, 27 June - 1 July 2022, Online, Maastricht, Netherlands, ECA Vol. 46A, O2.J503.
[8] M. Tanaka, H. Kato, N. Suzuki, et al., Removal of tritium from vacuum vessel by RF heated plasmas in LHD, Physica Scripta 96 (2021), 124007, https://doi.org/10.1088/1402-4896/ac1bf2.
[9] H.G. Esser, A. Lyssoivan, M. Freisinger, et al., ICRF wall conditioning at TEXTOR-94 in the presence of a 2.25 T magnetic field, J. Nucl. Mater. 241–243 (1997) 861–866, https://doi.org/10.1016/S0022-3115(97)80155-9.
[10] A. Hakola, S. Brezinsek, D. Douai, et al., Plasma-wall interaction studies in the full-W ASDEX upgrade during helium plasma discharges, Nucl. Fusion 57 (2017), 066015, https://doi.org/10.1088/1741-4326/aa69c4.
[11] E. Gauthier, E. de la Cal, B. Beaumont, et al., Wall conditioning technique development in Tore Supra with permanent magnetic field by ICRF wave injection, J. Nucl. Mater. 241–243 (1997) 553–558, https://doi.org/10.1016/S0022-3115(97)80098-0.
[12] Yaowei Yu, et al., ICRF (ion cyclotron range of frequencies) discharge cleaning with toroidal and vertical fields on EAST, Plasma Phys. Control. Fusion 53 (2011) 015013, https://doi.org/10.1088/0741-3335/53/1/015013.
[13] J.S. Hu, J.G. Li, Y.P. Zhao, He–ICR cleanings on full metallic walls in EAST full superconducting tokamak, J. Nucl. Mater. 376 (2008) 207–210, https://doi.org/10.1016/j.jnucmat.2008.02.090.
[14] Dong Su Lee, Suk-Ho Hong, Sungwoo Kim, et al., Ion Cyclotron Wall Conditioning (ICWC) on KSTAR, Fusion Eng. Des. 60 (2011) 94–97, https://doi.org/10.13182/FST11-A12412.
[15] T. Wauters, D. Matveev, D. Douai, et al., Isotope removal experiment in JET-ILW in view of T-removal after the 2nd DT campaign at JET, Physica Scripta 97 (2022), 044001, https://doi.org/10.1088/1402-4896/ac5856.
[16] J. Ongena, D. Castano-Bardawil, K. Crombe, et al., Physics design, construction and commissioning of the ICRH system for the stellarator Wendelstein 7-X, Fusion Eng. Des. 192 (2023) 113627, https://doi.org/10.1016/j.fusengdes.2023.113627.
[17] G.L. Ravera, S. Ceccuzzi, G. Granucci, et al., Operational requirements of the ion cyclotron wall conditioning in DTT, Fusion Eng. Des. 191 (2023), 113754, https://doi.org/10.1016/j.fusengdes.2023.113754.
[18] D. Douai, D. Kogut, T. Wauters, et al., Wall conditioning for ITER: Current experimental and modeling activities, J. Nucl. Mater. 463 (2015) 150–156, https://doi.org/10.1016/j.jnucmat.2014.12.034.
[19] A. Lyssoivan, D. Douai, R. Koch, et al., Simulation of ITER full-field ICWC scenario in JET: RF physics aspects, Plasma Phys. Control. Fusion 54 (2012), 074014, https://doi.org/10.1088/0741-3335/54/7/074014.
[20] T. Wauters, R. Bisson, E. Delabie, et al. Changeover between helium and hydrogen fuelled plasmas in JET and WEST. In: 19th International Conference on Plasma-Facing Materials and Components for Fusion Applications, 22 to 26 May, 2023, Bonn, Germany. ID: 309.
[21] A. Kaye, T. Brown, V. Bhatnagar, et al., Present and future JET ICRF antennae, Fusion Eng. Des. 24 (1994) 1–21, https://doi.org/10.1016/0920-3796(94)90034-5.
[22] M. Vrancken, M.-L. Mayoral, T. Blackman, Recent ICRF developments at JET, Fusion Eng. Des. 82 (2007) 873–880, https://doi.org/10.1016/j.fusengdes.2007.05.019.
[23] A Czarnecka, F. Durodié, A.C.A. Figueiredo, et al., Impurity production from the ion cyclotron resonance heating antennas in JET, Plasma Phys. Control. Fusion 54 (2012), 074013, https://doi.org/10.1088/0741-3335/54/7/074013.
[24] I. Monakhov, P. Jacquet, T. Blackman, et al., ICRH antenna S-matrix measurements and plasma coupling characterisation at JET, Nucl. Fusion 58 (2018), 046012, https://doi.org/10.1088/1741-4326/aaace3.
[25] M.K. Paul, A. Lyssoivan, R. Koch, et al., Plasma and antenna coupling characterization in ICRF-wall conditioning experiments, Fusion Eng. Des. 87 (2012) 98–103, https://doi.org/10.1016/j.fusengdes.2011.10.009.
[26] A. Boboc, C. Gil, P. Pastor, et al., Upgrade of the JET far infrared interferometer diagnostica, Rev. Sci. Instrum. 83 (2012) 10E341, https://doi.org/10.1063/1.4737420.
[27] A. Boboc, B. Bieg, R. Felton, et al., A novel calibration method for the JET real-time far infrared polarimeter and integration of polarimetry-based line-integrated density measurements for machine protection of a fusion plant, Rev. Sci. Instrum. 86 (2015), 091301, https://doi.org/10.1063/1.4929443.
[28] C.F. Maggi, S. Brezinsek, M.F. Stamp, et al., A new visible spectroscopy diagnostic for the JET ITER-like wall main chambera, Rev. Sci. Instrum. 83 (2012) 10D517, https://doi.org/10.1063/1.4733734.
[29] U. Kruezi, G. Sergienko, P.D. Morgan, et al., JET divertor diagnostic upgrade for neutral gas analysis, Rev. Sci. Instrum. 83 (2012) 10D728, https://doi.org/10.1063/1.4732175.
[30] U. Kruezi, I. Jepu, G. Sergienko, et al., Neutral gas analysis for JET DT operation, Journal of Instrumentation 15 (2020) C01032, https://doi.org/10.1088/1748-0221/15/01/C01032.
[31] M. Tripský, T. Wauters, A. Lyssoivan, et al., A PIC-MCC code RFdinity1d for simulation of discharge initiation by ICRF antenna, Nucl. Fusion 57 (2017), 126043, https://doi.org/10.1088/1741-4326/aa8446.
[32] T. Wauters, A. Lyssoivan, D. Douai, et al., 0D model of magnetized hydrogen–helium wall conditioning plasmas, Plasma Phys. Control. Fusion 53 (2011), 125003, https://doi.org/10.1088/0741-3335/53/12/125003.
[33] V. Moiseenko, Y.V. Kovtun, T. Wauters, et al., First experiments on ICRF discharge generation by a W7-X-like antenna in the Uragan-2M stellarator, J. Plasma Phys. 86 (2020) 905860517, https://doi.org/10.1017/S0022377820001099.
[34] S. Kamio, V.E. Moiseenko, Y.V. Kovtun, et al., First experiments on plasma production using field-aligned ICRF fast wave antennas in the large helical device, Nucl. Fusion 61 (2021), 114004, https://doi.org/10.1088/1741-4326/ac277b.

[35] V. Moiseenko, Y.V. Kovtun, A.V. Lozin, et al., Plasma Production in ICRF in the Uragan-2M Stellarator in Hydrogen-Helium Gas Mixture, J. Fusion Energ. 41 (2022) 15, https://doi.org/10.1007/s10894-022-00326-8.
[36] Y.V. Kovtun, V. Moiseenko, A.V. Lozin, et al., ICRF Plasma Production with the W7-X Like Antenna in the Uragan-2M Stellarator, Plasma Fusion Res. 17 (2022) 2402034, https://doi.org/10.1585/pfr.17.2402034.
[37] Y.V. Kovtun, V.E. Moiseenko, S. Kamio, et al., ICRF Plasma Production with Hydrogen Minority Heating in Uragan-2M and Large Helical Device, Plasma Fusion Res. 18 (2023) 2402042, https://doi.org/10.1585/pfr.18.2402042.